


## COMMUNICATION

# An anatomical study of the tibial nerve branches innervating the posterior tibial artery

Ren Lin<sup>1</sup>  | Geng Zhang<sup>1</sup> | Kai-yan Gan<sup>2</sup> | Yue-hong Zhuang<sup>1</sup>  |  
Rui-Min Pan<sup>2</sup> | Lin-bing Zou<sup>2</sup> | Yun Xie<sup>3</sup> | Xiao-zhen Zhao<sup>1</sup>

<sup>1</sup>Department of Human Anatomy, Laboratory of Clinical Applied Anatomy, School of Basic Medical Sciences, Fujian Medical University, Fuzhou, China

<sup>2</sup>2020 class (5+3 integrated) clinical medicine major, Fujian Medical University, Fuzhou, China

<sup>3</sup>Department of Orthopedics, The First Affiliated Hospital of Fujian Medical University, Fuzhou, China

## Correspondence

Xiao-zhen Zhao, Department of Human Anatomy, Laboratory of Clinical Applied Anatomy, School of Basic Medical Sciences, Fujian Medical University, No.1 Xuefu North Road, University Town, Fuzhou, Fujian Province 350122, China.  
Email: [zxz8338@163.com](mailto:zxz8338@163.com)

Yun Xie, Department of Orthopedics, The First Affiliated Hospital of Fujian Medical University, No.20 Cha-Zhong Road, Taijiang District, Fuzhou, Fujian Province 350005, China.  
Email: [xyxlr@126.com](mailto:xyxlr@126.com)

## Funding information

Clinical medicine ("5 + 3" integration) special scientific research training program of Fujian Medical University, Grant/Award Number: Kai-yan Gan

## Abstract

The arteries of the lower limbs are innervated by vascular branches (VBs) originating from the lumbar sympathetic trunk and branches of the spinal nerve. Although lumbar sympathectomy is used to treat nonreconstructive critical lower limb ischemia (CLLI), it has limited long-term effects. In addition, the anatomical structure of tibial nerve (TN) VBs remain incompletely understood. This study aimed to clarify their anatomy and better inform the surgical approach for nonreconstructive CLLI. Thirty-six adult cadavers were dissected under surgical microscopy to observe the patterns and origin points of VBs under direct vision. The calves were anatomically divided into five equal segments, and the number of VB origin points found in each was expressed as a proportion of the total found in the whole calf. Immunofluorescence staining was used to identify the sympathetic nerve fibers of the VBs. Our results showed that the TN gave off 3–4 VBs to innervate the posterior tibial artery (PTA), and the distances between VBs origin points and the medial tibial condyle were:  $24.7 \pm 16.3$  mm,  $91.7 \pm 66.1$  mm,  $199.6 \pm 52.0$  mm,  $231.7 \pm 38.5$  mm, respectively. They were mainly located in the first (40.46%) and fourth (31.68%) calf segments, and immunofluorescence staining showed that they contained tyrosine hydroxylase-positive sympathetic nerve fibers. These findings indicate that the TN gives off VBs to innervate the PTA and that these contain sympathetic nerve fibers. Therefore, these VBs may need to be cut to surgically treat nonreconstructable CLLI.

## KEYWORDS

arterial disease, posterior tibial artery, sympathectomy, tibial nerve

## 1 | INTRODUCTION

The main arteries of the lower limb include the femoral and popliteal arteries, anterior tibial artery, and posterior tibial artery (PTA). The PTA supplies the posterior region of the calf. It is continuous with the popliteal artery at the distal border of popliteus and gives off the fibular artery in the proximal part of the calf.

The nerve branches innervating the arteries are known as the vascular branches (VBs). Contraction of the arteries is regulated by

sympathetic nerves that originate from the sympathetic trunk and branches of the spinal nerves (Pick, 1958). VBs originating from the lumbar sympathetic trunk are frequently removed to relieve pain or salvage limbs when treating nonreconstructable critical lower limb ischemia (CLLI) caused by peripheral arterial occlusive disease (Batca et al., 2011; Karanth et al., 2016). Studies have shown that lumbar sympathectomy (LS) has a better early effect in the treatment of lower limb arterial occlusive disease, but the limb salvage rate in the second postoperative year is lower than that in the first year postoperatively

(Nemes et al., 2011). A retrospective study showed no difference in the efficacy between surgical and medical treatment for the occlusive peripheral arterial disease of the lower limbs (Ruiz-Aragon & Calderon, 2010). Moreover, the surgical efficacy is lower than that of drugs for improving pain or lower limb ulcers caused by CLLI (Sen et al., 2018).

Recently, VBs derived from spinal nerves have received increasing attention (Umemoto et al., 2018). These VBs of the spinal nerve have also been shown to contain sympathetic fibers, and stimulating their distribution can help treat peripheral circulatory failure in that area (Umemoto et al., 2020). These findings indicate that LS, which is currently performed clinically, has neither a complete nor near-complete inhibitory effect on the sympathetic fibers constricting the lower limb arteries.

The PTA is a predilection site for lower limb arterial occlusion (Anand et al., 2020; Firat & Igus, 2019). In addition, the tibial nerve (TN) is accompanied by the PTA. However, a TN origin of the VBs that innervate the PTA or their mode of innervation has not been reported in the literature. Therefore, this study aimed to clarify the anatomy of VBs from the TN innervating the PTA through the anatomical observation of cadaveric lower limbs and immunofluorescence staining, which may provide an anatomical basis to clinically improve the surgical management of nonreconstructable CLLI.

## 2 | MATERIALS AND METHODS

Thirty-six adult cadavers were dissected, including 24 males and 12 females, aged 45–65 years at death. The cadavers were donated to the Fujian Medical University, and their donors provided written informed consent for their use in experimental teaching and medical research before they died. This study complied with Chinese laws and was approved by the Ethics Committee of Fujian Medical University (Approval No.: 2022-112). The authors state that every effort was made to follow all local and international ethical guidelines and laws that pertain to the use of human cadaveric donors in anatomical research (Iwanaga et al., 2022). The cadavers were formalin-embalmed and fixed, and the exclusion criteria for the cadavers were the presence of any calf deformity and a history of surgery.

### 2.1 | Calf anatomy

Briefly, calf specimens were injected with a mixture of latex and red dye (ratio of 4:1) via the popliteal artery. The skin, superficial fascia, and deep fascia in the posterior area of the calf and popliteal fossa were sequentially removed. Next, the muscle was cut at the beginning of the triceps surae and turned downward, the posterior fascial septum of the calf was removed, and the PTA and TN were exposed. The TN crosses to the medial side of the PTA in the popliteal fossa and descends parallel to it to lie between the heel and medial malleolus. Subsequently, a scalpel handle was used to bluntly separate the TN in a craniocaudal direction, and its branches were initially exposed. The

VBs that reached the PTA were tracked and confirmed using a surgical microscope (Leica M690, Germany), and the posterior tibial vein was removed.

The upper edge of the medial tibial condyle (point A) and the highest point of the medial malleolus (point B) were used as the anatomical landmarks (Figure 1). Points A and B were connected to establish a measurement reference line, and the distance between them was also used to represent calf length. The origin of the VBs from the TN was defined as point C, and the distance from point A (AC) (unit: mm, accurate to one decimal place) was measured along the direction of the reference line with a digital Vernier caliper. The first point where the VBs reached the PTA was defined as point D, the end of the VBs as point E, and the distribution range of the VBs as the distance between them (DE). To exclude the influence of individual differences in the specimens, the AC/AB ratio was used as the relative position of the origin point of the VBs.

The calf length was divided into five equal parts according to the distance from the medial tibial condyle to the highest point of the medial malleolus (from proximal to distal, the first to the fifth segments) and the distribution of the origin points of all branches was counted.

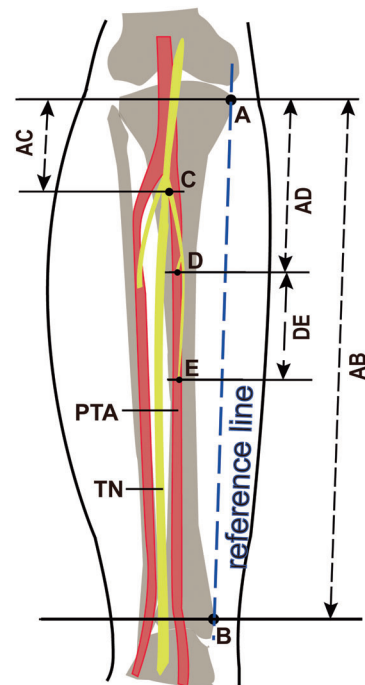


**FIGURE 1** Schematic of the vascular branches (VBs) of the tibial nerve (TN) measurements. (A) Medial tibial condyle; (B) The highest point of the medial malleolus; (C) The origin of the VB from the TN; (D) The first point of the VB reaching the PTA; and (E) The terminal end of the VB. A measurement reference line was made through the medial tibial condyle (A) and the highest point of the medial malleolus (B); AB: calf length; AC: the distance of the origin position of the VB from the medial tibial condyle; AD: the distance from the medial tibial condyle where the VB reaches the PTA; DE: the distribution range of the VB.

A ruler with 0.5 mm grid divisions and a total length of 1 cm was placed on the same plane as the VBs. After taking pictures with a camera (Sony HDR-PJ790E, Japan), the diameter of the VB trunks was measured using the ImageJ software (unit: mm, accurate to two decimal places). The above data were measured by three different researchers, and the mean value was calculated.

## 2.2 | Immunofluorescence staining

The PTA and its connected VBs were cross-sectioned at the point where the VBs reached the PTA (point D) at the center. After dehydration to the bottom with 20% and 30% sucrose, optimal cutting temperature compound embedding was performed, and continuous frozen sections were created along the long axis of the VB to include cross-sections of the blood vessel at a thickness of 50  $\mu$ m per piece.

Sections were washed three times in 0.01 M phosphate-buffer solution (PBS, pH 7.4) for 5 min; high-pressure antigen retrieval was performed using sodium citrate antigen repair solution at pH 6.0 for 15 min and washed with PBS. Subsequently, the sections were blocked with immunostaining blocking solution (Beyotime, China) at room temperature for 3 h and incubated with the rabbit anti-Tyrosine Hydroxylase antibody (TH; 1:500, Chemicon, USA) at 4°C for 72 h. PBS was used rather than the primary antibody as a negative control. After washing with PBS, the sections were incubated with donkey antirabbit IgG secondary antibody, Alexa flour 647 (1:500, Invitrogen, USA); and mouse antiactin, alpha-smooth muscle-Cy3 antibody ( $\alpha$ -SMA; 1:500, Millipore Sigma, USA) at room temperature for 3 h. Subsequently, after washing in PBS, the sections were spread on slides and sealed with an antifluorescence quencher. Finally, the three-dimensional reconstruction was performed after scanning using a laser confocal microscope (Leica TCS SP8, Germany) at a thickness of 2  $\mu$ m per layer.

## 2.3 | Statistical analysis

IBM SPSS version 19.0 (IBM Corp., USA) software was used for the data analysis. Measurement data were expressed as means  $\pm$  standard deviation ( $\bar{x} \pm s$ ), and differences between groups were analyzed using a *t*-test, and *p* < 0.05 was considered statistically significant.

# 3 | RESULTS

## 3.1 | Branching pattern of the VBs from the TN

All VBs innervating the PTA were derived from the TN. There were three (36.1%) or four (63.9%) VBs to the PTA, which were defined as the first, second, third, and fourth branches from the proximal to the distal end. No significant differences were found in the number of branches between the sexes or calves on different sides (*p* > 0.05).

Three patterns of VB emanating from the TN were identified as follows: independent trunk type (type I), common trunk type (type II),

and muscular branch type (type III) (Figure 2). Type I was defined as the main trunk of the VB originating from the TN alone, with all or most of the branches supplying the PTA. In type II, the VB and muscle branch had a cotrunk starting from the TN which then divided into two or more branches, with one supplying the PTA and the others supplying the muscles in the posterior region of the calf. In type III, the main trunk of the VB originated from the muscular branch of the TN.

Among the 72 calves observed, 60 specimens showed type II (28/72) and type III (32/72) branches, of which 8 calves had type II coexisting with type III, and all VBs of the remaining 12 calves were type I (12/72). For each branch, types II and III of the first branches accounted for 36.1% and 27.8%, respectively; types II and III of the second branches were both 19.4%; and the third branches were all type I. Calves that had the fourth branch with patterns of types II and III only accounted for 5.6% and 2.8% of all calves observed, respectively. In addition, those with a branch trunk diameter of more than 1.25 mm were more likely to be type II or III.

The muscle branches of types II and III mainly innervate the deep posterior group of calf muscles. Among them, the flexor digitorum longus (45.5%) was the most common, followed by the flexor hallucis longus (27.3%), the tibialis posterior (9%) was the least common, and 18.2% of type II or III branches innervated both the flexor hallucis longus and tibialis posterior.

The TN was observed to have five branch patterns based on the morphological differences between its branches to the PTA (Figure 3). Among all the branch patterns, type C (5.7%) had the lowest occurrence rate, whereas types A, B, D, and E had occurrence rates of 20.5%, 20.5%, 25.4%, and 27.9%, respectively.

## 3.2 | Origin and course of the VBs from the TN

Of all VBs observed, 93.1% (244/262) originated from the TN on the side closest to the PTA, and only 6.9% (mainly in the first branch) originated from the TN on the side furthest from the PTA. The origins of the first branch were relatively constant and located at  $24.7 \pm 16.3$  mm below the medial tibial condyle, which was  $7.6 \pm 5.0$  (%) of the calves. The origins of the second, third, and fourth branches were located at  $91.7 \pm 66.1$  mm,  $199.6 \pm 52.0$  mm, and  $231.7 \pm 38.5$  mm below the medial tibial condyle, and  $28.2 \pm 20.7$  (%),  $60.7 \pm 15.8$  (%) and  $70.1 \pm 11.4$  (%), according to the relative position of the lower leg, respectively (Table 1). In the calves with four VBs (*n* = 46), the second branch was closer to the first branch, and the distance between them was  $26.6 \pm 16.6$  mm, while the third branch was at a distance similar to that of the second branch of calves with three VBs. In addition, 52.7% of the VBs entered the PTA from the fibular side, followed by 17.6% from the posterior side.

Analysis of the VB distribution within the calf revealed the proportions of all VB origin points located within each segment. These results showed that the first branch origin was mainly located in segment 1 (94.4%, 68/72); the second branch origin was located mostly in segment 1 (52.8%, 38/72), followed by segment 2 (20.8%, 15/72) and segment 4 (18.1%, 13/72); the third branch mainly originated

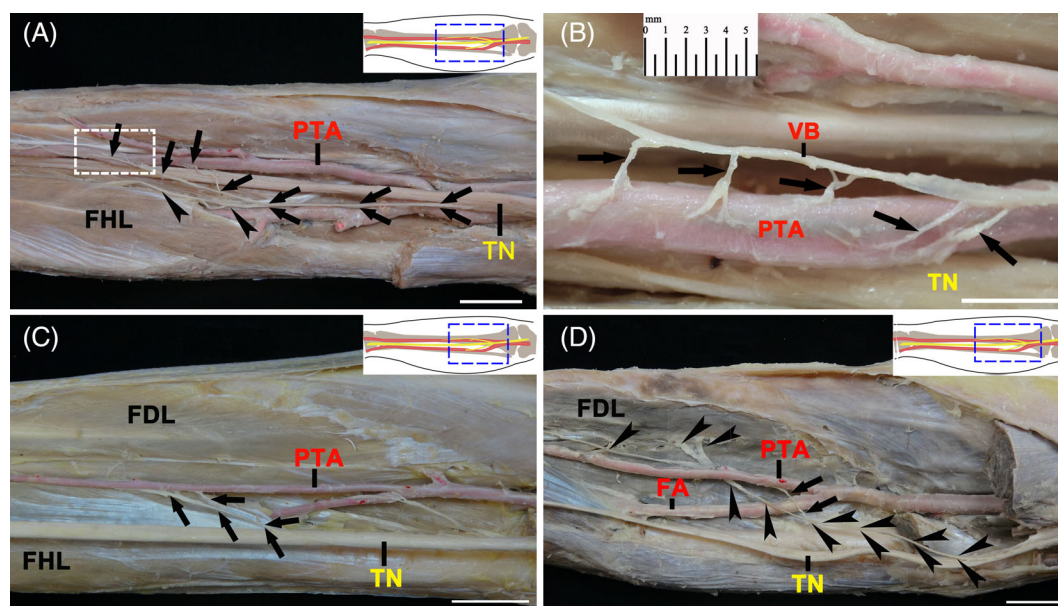


**FIGURE 2** Branch patterns of the vascular branches (VBs) from the tibial nerve (TN). (A) A common trunk VB. The figure shows that the branch trunk descends from the fibular side of the TN and then divides into two branches. One branch runs obliquely toward the tibial side and is distributed on the PTA, whereas the other runs on the fibular side and is distributed on the FHL. (B) A partially enlarged picture of the VB in (A) (Frame Selected Area) after pulling showing that the VB sends out small branches to innervate the PTA. (C) An independent trunk type VB. The nerve branch from the TN runs obliquely to the tibial side and is divided into two branches distributed in the PTA. (D) A muscular branch type VB. In this figure, the main branch emanates from the TN and runs obliquely to the tibial side. Before crossing the FA, one branch is distributed in the PTA, and the main branch is divided into three branches and distributed in the FDL after crossing the PTA. Long-tailed arrows indicate the main trunk and VB, and the triangular arrows indicate the muscle branch. Bar = 0.5 mm (B) or 2 cm (A, C, D). FA, fibular artery; FDL, flexor digitorum longus; FHL, flexor hallucis longus; PTA, posterior tibial artery.

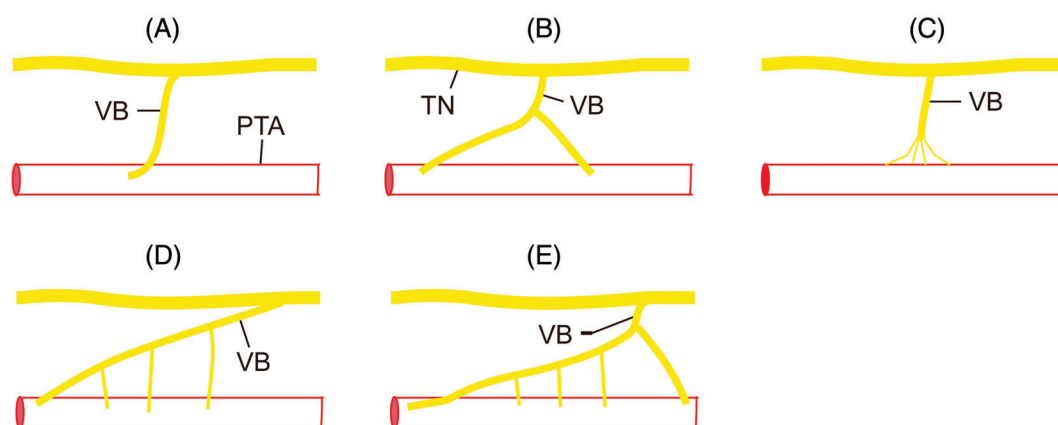


**FIGURE 3** Schematic diagram of the domination pattern of vascular branches (VBs) of the posterior tibial artery (PTA). Type A (single-trunk type): the trunk of the VB does not have ramifications before reaching the PTA; Type B (double-branch type): the trunk of the VB is divided into two branches before reaching the PTA, but these two branches have no secondary branches before entering the artery; Type C (claw type): the trunk of the VB is divided into several small branches before reaching the PTA. Type D (long-trunk type): the trunk of the VB is a long branch, which gives off several secondary branches into the artery before descending to the PTA; Type E (mixed type): that is, long trunk–single trunk–mixed type, the trunk of the VB before reaching the PTA is divided into two branches, one of which is the long-trunk type, the other is the single-trunk type. TN, tibial nerve.

from segment 4 (68.1%, 49/72), followed by segment 2 (22.2%, 16/72); and the fourth branch origin was located mostly in segment 4 (45.7%, 21/46), followed by segment 3 (32.6%, 15/46). In conclusion, the VBs of the TN originating from the first, fourth, and fifth segments accounted for 40.46% (106/262), 31.68% (83/262), and 3.82%, respectively (Figure 4).

### 3.3 | Distribution and diameter of the VBs from the TN in the PTA

The distance from the first point of the VB reaching the PTA to its endpoint was defined as the distribution range. The results showed that the distribution range of VBs varied greatly, with the shortest,



**TABLE 1** Ramifications of the vascular branches (VBs) innervating the posterior tibial artery

The branches	AC (mm)	AB (mm)	AC/AB(%)	AD (mm)	The diameter of VBs (mm)	n (%)
First	24.7 ± 16.3	329.4 ± 16.8	7.6 ± 5.0	80.3 ± 15.9	1.18 ± 0.36	72/72 (100%)
Second	91.7 ± 66.1	329.4 ± 16.8	28.2 ± 20.7	152.2 ± 77.0	0.98 ± 0.43	72/72 (100%)
Third	199.6 ± 52.0	329.4 ± 16.8	60.7 ± 15.8	221.2 ± 54.0	0.72 ± 0.22	72/72 (100%)
Fourth	231.7 ± 38.5	329.4 ± 16.8	70.1 ± 11.4	242.8 ± 38.7	1.00 ± 0.58	46/72 (63.9%)

Note: AC: distance from the medial tibial condyle to the origin point of the VBs; AB: distance from the medial tibial condyle to the medial malleolus; AD: distance from the medial tibial condyle to the first position where the VBs reach the posterior tibial artery.

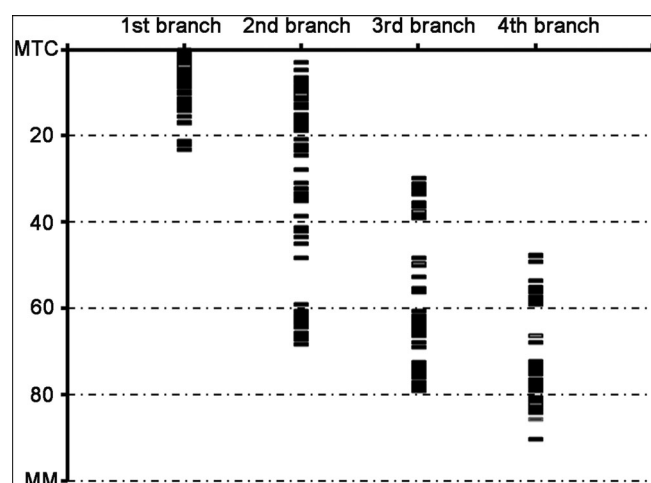


**FIGURE 4** Distribution of the origin point of the vascular branches from the tibial nerve in each segment of the calf. The length of the calf is divided into five equal parts according to the distance from the MTC to the highest point of the MM, from proximal to distal. These are the first to fifth segments, respectively. Notably, 94.4% of the first branch started from segment 1 of the calf (68/72). Regarding the second branch, 52.8% started from segment 1 (38/72), and 20.8% and 18.1% started from segment 2 (15/72) and segment 4 (13/72), respectively. The third branch mainly started from the fourth segment of the calves (68.1%, 49/72), followed by the second segment (22.2%, 16/72). Moreover, 45.7% of the fourth branch originated from the fourth segment (21/46), followed by 32.6% from the third segment (15/46). MM, medial malleolus; MTC, medial tibial condyle.

longest, and median being 2.2, 216.5, and 85.23 mm, respectively. In addition, the ends of the third or fourth branches perforated into the tarsal tunnel in 61.1% of calves.

The mean diameters of the first to fourth branches were  $1.18 \pm 0.36$  mm,  $0.98 \pm 0.43$  mm,  $0.72 \pm 0.22$  mm, and  $1.00 \pm 0.58$ , respectively. The mean diameter of the VBs of types II and III was  $1.25 \pm 0.38$  mm, whereas that of type I VBs was  $0.85 \pm 0.38$  mm (Table 1).

### 3.4 | The VBs contain sympathetic nerve fibers

Immunofluorescence staining results showed that  $\alpha$ -SMA-positive smooth muscle fibers were expressed in the arterial wall in a cord-like

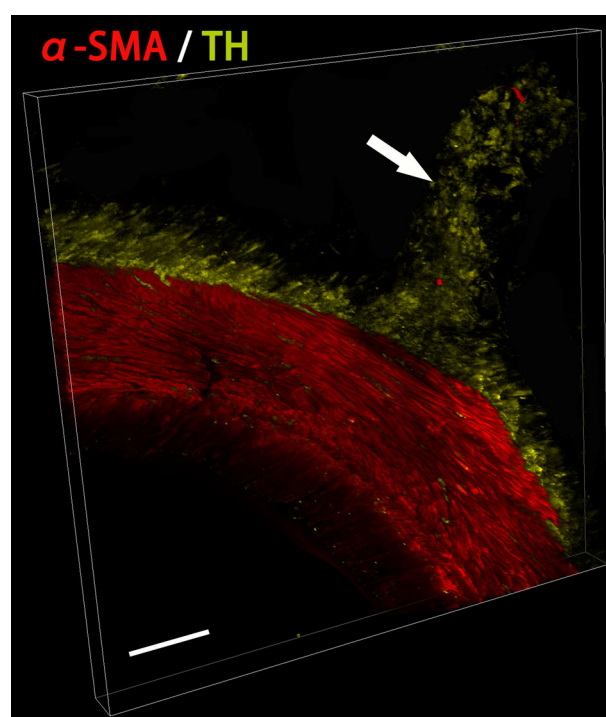


**FIGURE 5** Immunofluorescence staining with alpha-smooth muscle-Cy3 antibody ( $\alpha$ -SMA) and tyrosine hydroxylase (TH) of a posterior tibial artery (PTA) and vascular branch frozen section.  $\alpha$ -SMA (red) and TH (yellow) represent the PTA wall and sympathetic nerve fibers, respectively. The TH-labeled vascular branch (arrow) moves toward the PTA and connects with sympathetic nerve fibers located at the periphery of the artery wall. Bar = 100  $\mu$ m.

manner, forming a curved structure (Figure 5). Sympathetic fibers with TH-positive markers, which were observed around the arterial wall, were radially expressed, forming an arc-shaped structure that adhered to the surface of the arterial wall. Some TH-positive sympathetic fibers penetrated the arterial wall in a cord or dot shape or were scattered in the arterial wall for expression. In addition, many TH-positive sympathetic fibers were expressed in the VB and were connected to the sympathetic fibers in the periphery of the arterial wall.

## 4 | DISCUSSION

In this study, 72 calves were anatomically observed, and it was clear that the TN supplied three or four VBs to innervate the PTA.

Immunofluorescence staining showed that these VBs contained sympathetic fibers and were connected to those distributed around the PTA. This result is consistent with the existing view that the nerves innervating the arteries contain sympathetic fibers.

LS is a typical procedure for treating arterial occlusion of the lower limbs. However, its long-term effects are limited (Nemes et al., 2011; Ruiz-Aragon & Calderon, 2010), possibly because VBs innervate the lower limb arteries from two groups of nerves: the lumbar sympathetic trunk and the lumbosacral plexus. Moreover, LS cannot block the VBs from the lumbosacral plexus. This study provides an anatomical theory for performing LS while cutting off VBs derived from the TN. Because of the different branching patterns of the VBs in the PTA and the large differences in the range of their innervation, the point where the VBs reach the PTA is unsuitable for the surgical approach. Specifically, this study focused on measuring the positions of origin of the VBs. It was found that the original position of the first branch was relatively constant, that is,  $24.7 \pm 16.3$  mm below the medial tibial condyle. In addition, the distance between the second and first branches of the calves with four branches was smaller than that of calves with only three branches. It was also found that the origin points of the VBs were mainly located in the first (40.46%) and fourth (31.68%) segment of the calf, and the VBs from the fifth were the least common (3.82%).

In addition to the VBs found in this study, the TN branches mainly supply muscles in the posterior region of the calf and the plantar muscles (Desai & Cohen-Levy, 2022). We found that some VBs originated from the common trunk with muscle branches or the muscle branches, with the first branch (63.9%) being the most common, followed by the second branch (38.8%), and the muscles innervated are most commonly flexor hallucis longus and flexor digitorum longus. Therefore, it is necessary to inadvertently avoid severing the above muscle branches when cutting the first and second branches. Furthermore, the branch trunk diameter can be used as a reference, and a branch trunk diameter of more than 1.25 mm is more likely to be a common trunk or muscle branch type.

In conclusion, the VBs of the TN are an important group of nerves that innervate the PTA. The first and fourth segments of the calf are the areas where the origin points of the VBs are concentrated and may be used as surgical approaches to cut off these VBs. However, 27.86% of VBs outside these two segments may not be surgically severed, and their effect on surgical outcomes needs further study.

## ACKNOWLEDGMENTS

The authors sincerely thank those who donated their bodies to science so that anatomical research could be performed. Results from such research can potentially increase mankind's overall knowledge can then improve patient care. Therefore, these donors and their families deserve our highest gratitude (Iwanaga et al., 2021). We also thank the Public Technical Service Center of Fujian Medical University for its support with laser confocal photography.

## ORCID

Ren Lin  <https://orcid.org/0000-0002-3739-0204>

Yue-hong Zhuang  <https://orcid.org/0000-0003-3997-7663>

## REFERENCES

- Anand, G. M., Conway, A. M., & Giangola, G. (2020). Single versus multiple vessel endovascular tibial artery revascularization for critical limb ischemia: A review of the literature. *International Journal of Angiology*, 29(3), 175–179. <https://doi.org/10.1055/s-0040-1714662>
- Batca, V., Jitea, N., Albita, O., Bitca, T., & Manuc, D. (2011). The efficiency of lumbar transperitoneal laparoscopic sympathectomy-100 cases revue. *Chirurgia*, 106(5), 591–597.
- Desai, S. S., & Cohen-Levy, W. B. (2022). *Anatomy, bony pelvis and lower limb, tibial nerve*. StatPearls.
- Firat, A., & Igus, B. (2019). Combined percutaneous direct puncture of occluded artery – antegrade intervention for recanalization of below the knee arteries. *Diagnostic and Interventional Radiology*, 25(4), 320–327. <https://doi.org/10.5152/dir.2019.18580>
- Iwanaga, J., Singh, V., Ohtsuka, A., Hwang, Y., Kim, H. J., Morys, J., Ravi, K. S., Ribatti, D., Trainor, P. A., Sanudo, J. R., Apaydin, N., Sengul, G., Albertine, K. H., Walocha, J. A., Loukas, M., Duparc, F., Paulsen, F., Del Sol, M., Addis, P., ... Tubbs, R. S. (2021). Acknowledging the use of human cadaveric tissues in research papers: Recommendations from anatomical journal editors. *Clinical Anatomy*, 34(1), 2–4. <https://doi.org/10.1002/ca.23671>
- Iwanaga, J., Singh, V., Takeda, S., Ogeng'o, J., Kim, H. J., Morys, J., Ravi, K. S., Ribatti, D., Trainor, P. A., Sanudo, J. R., Apaydin, N., Sharma, A., Smith, H. F., Walocha, J. A., Hegazy, A. M. S., Duparc, F., Paulsen, F., Del Sol, M., Addis, P., ... Tubbs, R. S. (2022). Standardized statement for the ethical use of human cadaveric tissues in anatomy research papers: Recommendations from anatomical journal editors-in-chief. *Clinical Anatomy*, 35(4), 526–528. <https://doi.org/10.1002/ca.23849>
- Karanth, V. K. L., Karanth, T. K., & Karanth, L. (2016). Lumbar sympathectomy techniques for critical lower limb ischaemia due to non-reconstructable peripheral arterial disease. *Cochrane Database of Syst Rev*, 12(12), CD011519. <https://doi.org/10.1002/14651858.CD011519.pub2>
- Nemes, R., Surlin, V., Chiutu, L., Georgescu, E., Georgescu, M., & Georgescu, I. (2011). Retroperitoneoscopic lumbar sympathectomy: Prospective study upon a series of 50 consecutive patients. *Surgical Endoscopy and Other Interventional Techniques*, 25(9), 3066–3070. <https://doi.org/10.1007/s00464-011-1671-8>
- Pick, J. (1958). The innervation of the arteries in the upper limb of man. *The Anatomical Record*, 130(1), 103–123. <https://doi.org/10.1002/ar.1091300109>
- Ruiz-Aragon, J., & Calderon, S. M. (2010). Effectiveness of lumbar sympathectomy in the treatment of occlusive peripheral vascular disease in lower limbs: Systematic review. *Medicina Clinica*, 134(11), 477–482. <https://doi.org/10.1016/j.medcli.2009.09.039>
- Sen, I., Agarwal, S., Tharyan, P., & Forster, R. (2018). Lumbar sympathectomy versus prostanoids for critical limb ischaemia due to non-reconstructable peripheral arterial disease. *Cochrane Database of Systematic Reviews*, 4(4), CD009366. <https://doi.org/10.1002/14651858.CD009366.pub2>
- Umemoto, K., Naito, M., Hatayama, N., Hirai, S., & Sakabe, K. (2020). A part of the medial branch of the deep peroneal nerve distributes the dorsal pedis artery and its distribution area is close to the acupuncture point LR3 (Taichong). *Evidence-based Complementary and Alternative Medicine*, 2020, 6760958. <https://doi.org/10.1155/2020/6760958>
- Umemoto, K., Ohmichi, M., Ohmichi, Y., Yakura, T., Hammer, N., Mizuno, D., Naito, M., & Nakano, T. (2018). Vascular branches from cutaneous nerve of the forearm and hand: Application to better understanding raynaud's disease. *Clinical Anatomy*, 31(5), 734–741. <https://doi.org/10.1002/ca.22993>

**How to cite this article:** Lin, R., Zhang, G., Gan, K., Zhuang, Y., Pan, R.-M., Zou, L., Xie, Y., & Zhao, X. (2022). An anatomical study of the tibial nerve branches innervating the posterior tibial artery. *Clinical Anatomy*, 1–6. <https://doi.org/10.1002/ca.23997>